

# First Results of the 74 MHz VLA-Pie Town Link. Hercules A at Low Frequencies

Nectaria A. B. Gizani,<sup>1,2</sup> <sup>\*</sup>, A. Cohen,<sup>3</sup> and N. E. Kassim,<sup>3</sup>

<sup>1</sup> *Grupo de Astrofísica da Universidade de Coimbra e Observatório Astronómico da Universidade de Coimbra, Santa Clara, 3040 Coimbra, Portugal*

<sup>2</sup> *Institute of Astronomy and Astrophysics, National Observatory of Athens, I. Metaxa & B. Pavlou, Lofos Koufou, Palaia Penteli, 15236 Athens, Greece.*

<sup>3</sup> *Naval Research Laboratory, Code 7213, Washington, DC 20375, USA*

26 June 2018

## ABSTRACT

We present the results of the first successful observations of the Pie Town link with the Very Large Array (VLA) at 74 MHz on Hercules A. The improvement in resolution from 25 arcsec to 10 arcsec resolves the helical- and ring-like features seen at higher frequencies. We also present new high dynamic range images of this powerful radio galaxy at 325 MHz. Our low frequency observations confirm the multiple outburst interpretation of the spectral index differences at high frequencies. Comparison between our radio and ROSAT X-ray data does not reveal any association between the X-ray emission from the cluster and the radio lobes. There are no extra regions of radio emission at 74 MHz.

**Key words:** galaxies: active; radio continuum: galaxies; galaxies: individual (Hercules A); clusters: individual (the Hercules A cluster); methods: data analysis; techniques: image processing

## 1 INTRODUCTION

### 1.1 Hercules A

Hercules A (Her A) is a complex extended radio galaxy at a low redshift of  $z = 0.154$  (see Gizani & Leahy 2004, 2003 for a review on this source and results from new observations). It is one of the most luminous radio sources in terms of apparent and intrinsic brightness. Its total power output is nearly as great as Cygnus A. At low frequency, it is one of the brightest radio sources in the sky at 170 and 800 Jy at 325 (VLA P-band) and 74 MHz (VLA 4-band) respectively (Kassim et al. 1993). Its total radio luminosity is  $\sim 3.8 \times 10^{37}$  W in the band 10 MHz to 100 GHz<sup>1</sup>. Hercules A is classified as an FR1.5 (Dreher & Feigelson 1984). With a linear size of 540 kpc and a width of  $\simeq 250$  kpc (angular size =  $194 \times 70$  arcsec), this radio galaxy possesses an unusual jet-dominated morphology, almost symmetrically extended

lobes and no compact hotspots. The ring-like/helical features on both sides of the radio emission form an almost symmetrical sequence which suggests successive ejections from the active nucleus (Gizani & Leahy 2003).

Her A has also been studied in the X-rays with the ROSAT PSPC (Position Sensitive Proportional Counter) and HRI (High Resolution Imager) (Gizani & Leahy 2004). The cluster is luminous in X-rays with a bolometric luminosity  $L_{\text{bol}} = 4.8 \times 10^{37}$  W. Her A itself lies at the center of the cluster, which should also have a cooling flow at the center, when the powerful jets are absent. Currently, however, it is critically disturbed by the expansion of the radio lobes. The PSPC spectrum reveals a cool component of the intraluster medium (ICM) with  $kT = 2.52$  keV. The total mass of the cluster is estimated to be  $1.5 \times 10^{14} M_{\odot}$ .

Gizani & Leahy (2003), have made an extensive study of Her A with the VLA 1.4 GHz band (L-band, A-, B-, C- configuration) at 1295, 1364.9, 1435.1, and 1664.9 MHz; 8.4 GHz band (X-band, B-, C-, D- configuration) at 8414.9 and 8464.9 MHz and reprocessed the 5 GHz band data (C-band, B-, C- and D- configuration) at 4872.6 MHz by Dreher & Feigelson (1984). Gizani & Leahy 2003, have produced a spectral index map with 1.4 arcsec resolution which provided a detailed picture of the plasma throughout the complex morphology, and gave a fairly good idea about the

<sup>1</sup> We use  $H_0 = 65 \text{ kms}^{-1} \text{ Mpc}^{-1}$  and  $q_0 = 0$  throughout for consistency with the series of papers on this object. We are not very wrong in doing this, since the recent WMAP (Wilkinson Microwave Anisotropy Probe, Bennett et al. 2003) data give  $H_0 = 71 \text{ kms}^{-1} \text{ Mpc}^{-1}$  and  $q_0 = -0.595$ , which do not change our results significantly.

temporal history of the plasma. Clearly the spectral index map separates the source in distinct regions of brighter, flatter (younger material) and fainter, steeper (older material), which is some evidence for spectral curvature, suggesting that we may be witnessing a renewed outburst from the active nucleus (Gizani & Leahy 2003). Generally spatial and spectral variations in a source imply temporal variations as well (Leahy 1991).

However the multifrequency measurements of Gizani & Leahy (2003) contained data from only a relatively small frequency range (1.4 to 8.4 GHz), with each one of the four frequencies of the 1.4 GHz band, not very far apart from each other. More quantitative conclusions, such as estimating the aging of Her A require a much wider frequency range which extends to low enough frequencies to map the break frequency throughout this radio galaxy. Low frequencies are more likely to trace the shape of the injected spectrum, before the aging effects have introduced spectral breaks. With this goal in mind, we have observed Her A at both 325 and 74 MHz.

The archived VLA data, at these frequencies are of low resolution and especially the 74 MHz data are poor. Fig. 1 shows contours of the old maps of Her A at 74 (top) and 325 MHz (bottom). Gizani & Leahy (2003) have also found the faint extended emission ‘cocoon’, at 1.4 GHz, 1.4 arcsec resolution, surrounding the core and jets of Her A shown in Fig. 1 (see also Kassim et al. 1993).

It is clear that even in the A-configuration, the VLA does not have the resolution required at 74 MHz to provide a useful spectral index map. Therefore, we turn to the most recent advance in high-resolution, low-frequency observations, the VLA-Pie Town link, which has just been upgraded to operate at 74 MHz.

### 1.2 The VLA-Pie Town Link at 74 MHz

In spite of the importance that low frequencies ( $\nu \leq 100$  MHz) have played in the discovery and development of radio astronomy (Jansky 1933, Reber 1940, Ryle & Smith 1948, Hewish 1952), the region of the electromagnetic spectrum below 100 MHz remains among the most poorly explored, despite its great scientific potential. While interferometers such as MERLIN (Multi Element Radio Linked Interferometer) have brought higher resolution interferometry to frequencies as low as 151 MHz (resolution 3 arc-second), sub-arcminute imaging below 100 MHz has been limited because ionospheric phase fluctuations have restricted interferometer baselines to  $\sim 5$  km (see for example Erickson et al. (1982) and Rees (1990)). The resulting poor angular resolution and consequently confusion limited sensitivity have left frequencies below 100 MHz in a seeming dark ages relative to centimeter wavelength radio astronomy that can exploit the long baselines ( $\geq 35$  km) of instruments such as the VLA, MERLIN, and the VLBA. An important breakthrough was the demonstration that the technique of self-calibration could mitigate the ionospheric limitations and thereby achieve sub-arcminute resolution imaging at the longer wavelengths (Kassim et al. 1993). During the 1990s, the National Radio Astronomy Observatory (NRAO) and Naval Research Laboratory (NRL) developed 74 MHz system at the VLA was the first connected element imaging array to successfully break the ‘ionospheric barrier’ below

100 MHz by achieving  $\sim 20$  arcsec resolution at 74 MHz. In 2001, NRL and NRAO collaborated again to develop a 74 MHz observing system on the Pie Town VLBA antenna (hereafter PT) located 50 km from the center of the VLA and linked to it via optical fiber. In 2002 the first successful fringes were obtained at both 74 and 330 MHz on the radio galaxy 3C 123, thereby marking another important step forward in the development of high angular resolution, low frequency imaging.

Today, low frequency systems on the VLA and the Giant Metrewave Radio Telescope (GMRT) are creating a quiet renaissance in long wavelength radio astronomy, producing high angular resolution, high sensitivity images (Kassim et al. 2004) and stimulating the development of instruments with even greater capability (e.g. Low Frequency Array (LOFAR), see Kassim et al. (2002)).

In this paper we present the first successful scientific observations of a cosmic radio source, the powerful FR I/II radio galaxy Her A, using the new VLA+PT system, thereby achieving the highest angular resolution image ever obtained by a connected element interferometer at a frequency below 100 MHz.

### 1.3 Outline of Paper

We present the total intensity map of Her A at 74 MHz employing the VLA-PT link, the corresponding map at 325 MHz as well as the spectral index map between 74 and 325 MHz. The spectral imaging analysis in the frequency range (0.074 to 8.4 GHz) and the resulting spectral aging study will be presented in a subsequent paper. Section 2 details the observations we made and Section 3 describes the data reduction and analysis. Results are discussed in Section 4 and in Section 5 we summarise our conclusions.

## 2 OBSERVATIONS

We have used the NRAO’s VLA to obtain total intensity images of Her A at both 325 and 74 MHz, in order to make a spectral aging study. As the limiting factor in creating an accurate spectral index map of this source is the low resolution obtainable at 74 MHz, we employed the new VLA-PT link to increase the resolution at that frequency. At 325 MHz, we observed both in the A and B-configurations in order to maintain both high resolution and sensitivity to the large scale source structure. At 74 MHz, we are restricted to 1.5 MHz bandwidth, because that is the only part of the frequency spectrum in that region that is protected for astronomy. At 325 MHz we chose the 6.25 MHz bandwidth, because this is the maximum that the correlator can handle while still having channels narrow enough to avoid bandwidth smearing.

We observed in the multichannel continuum mode in order to reduce the effects of bandwidth smearing and to more efficiently remove radio frequency interference (RFI). In the A-configuration, we observed both frequencies, 325 and 74 MHz, simultaneously, each in a separate IF. In the B-configuration, we only observed in the 325 MHz band, and we observed in two IF settings (328.5 and 321.5625 MHz). The observations contained nearly full tracks, necessary to maximise the  $uv$ -coverage so that we could map the complex

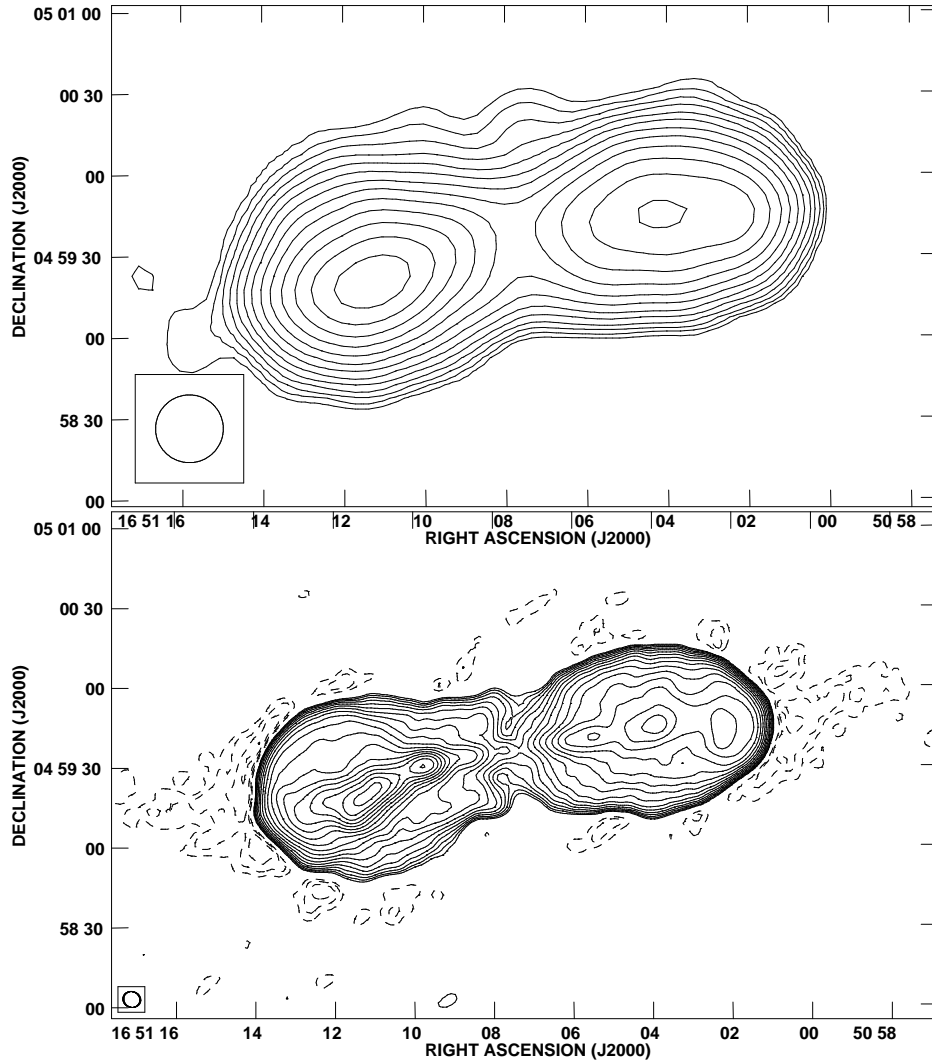


**Figure 1.** Top: Snapshot image at 74 MHz A-array with only 8 antennas. The peak brightness is  $119 \text{ Jy beam}^{-1}$ , the rms noise is  $0.5 \text{ Jy beam}^{-1}$  and the resolution is  $25 \times 25 \text{ arcsec}$ . Contours are logarithmic separated by factors  $\sqrt{2}$ . The first contour is at  $1.5 \text{ Jy beam}^{-1}$ . Bottom: Snapshot image at 325 MHz. The peak brightness is  $6.3 \text{ Jy beam}^{-1}$ , the rms noise is  $3.7 \text{ mJy beam}^{-1}$  and the beam is  $6.47 \times 5.87 \text{ arcsec}$  with position angle  $\text{PA} = 67.5 \text{ deg}$ . As before, contours are logarithmic separated by factors  $\sqrt{2}$  starting at  $15 \text{ mJy beam}^{-1}$ . In both figures coordinates are given in the Julian J(2000) coordinate system to match our new maps.

**Table 1.** Observations of Her A.

Config	Frequency MHz	Bandwidth MHz	Channels #	IFs #	Time hrs	Dates
A + PT	74	1.56	64	1	8	April 2002
A	325	6.25	16	1	8	April 2002
B	325	6.25	16	2	4	August 2002

structure of Her A. Full details of the observations are given in Table 1.

Cygnus A (Cyg A) was used as a bandpass calibrator at both frequencies. As Cyg A is resolved at both frequencies, accurate source models were required for calibration at each frequency, which are also available online<sup>2</sup>. For the 74 MHz model of Cyg A, we have used a high resolution

( $\sim 9 \text{ arcsec}$ ) image produced with the PT link only about 2 weeks before our own observations (Kassim, Carilli, Harris and Perley, private communication). For the 325 MHz model of this source we have made use of the model available in the on-line low-frequency data reduction tutorial (see Section 3).

For flux calibrators, we used 3C 286 and Cyg A for 325 and 74 MHz respectively. For Cyg A again we used the model, because of the resolved source structure, restricting to inner channels. For 3C 286, which is unresolved at

<sup>2</sup> <http://lofar.nrl.navy.mil/pubs/tutorial/node49.html>

this frequency and resolution, we did not require a model for calibration. No phase calibrator was observed, because with the high amount of flux density in Her A we determined that self-calibration would be sufficient for this purpose. Approximately 90 per cent of the time was spent on the target source, the remainder on calibrators and slewing.

The observations went almost as planned. Some of the 74 MHz data were affected by interference and unstable rack temperatures, and data of the 325 MHz were occasionally lost for other reasons including antenna motor faults. The total downtime per antenna was 10.3 minutes.

### 3 DATA REDUCTION & ANALYSIS

The greatest difficulty in the data reduction at low frequencies comes from the non-coplanar array geometry and the large field of view (f.o.v.) of the VLA. For the reducing and imaging of the data we have used routines in the Astronomical Image Processing Software (AIPS). We have largely followed the methodology described by T. J. W. Lazio, N. E. Kassim, & R. A. Perley in “Low-Frequency Data Reduction at the VLA: A Tutorial for New Users”, also found on-line<sup>3</sup>.

After performing bandpass (using Cyg A) and flux calibration (using Cyg A at 74 MHz and 3C286 at 325 MHz), excision of RFI was performed by first clipping all data points well above the actual flux in the image. Our clip levels were 300 and 5,000 Jy/beam for 325 MHz and 74 MHz respectively. Once the worst RFI was removed from the channel data, we averaged the channels as far as possible without introducing bandwidth smearing (aips task SPLAT). At 325 MHz, we averaged the entire bandwidth to a single channel per IF. At 74 MHz, we took the central 56 channels out of the original 64 and averaged this down to 7 channels. After channel averaging, additional RFI flagging was performed by hand (aips task TVFLG).

#### 3.1 Mapping

The full f.o.v. , defined roughly by the primary beam area, has a diameter of  $2.5^\circ$  and  $11.5^\circ$  for 325 and 74 MHz respectively. However, because Her A is one of the brightest objects in the sky, it completely dominates all other sources in the field, making it unnecessary to clean other sources in the primary beam area. Therefore, only a small region surrounding Her A (size  $\sim 3$  arcmin) needed to be imaged, removing the need for the usual “fly’s eye” approximation<sup>4</sup> to the three-dimensional Fourier inversions necessary to map the entire primary beam area.

For the 325 MHz data, we combined the A-configuration and B-configuration data in the  $uv$  plane before imaging (aips task DBCON). For the 74 MHz data, we have included PT link data, which increases the maximum baseline to 73 km. However, the coverage of the outer regions of the  $uv$ -plane, provided by the VLA-PT baselines, is sparse and elongated nearly east-west (Fig. 3) This is due to the near

equatorial location of Her A ( $\delta \simeq 5^\circ$ ), and results in a highly elongated synthesised beam. Imaging was performed for each frequency with a nearly uniform weighting (robust factor of  $-2$ ) and with 1.5 arcsec pixels (aips task IMAGR). Several rounds of phase-only self-calibration were performed on each data set until the map noise stopped decreasing (aips task CALIB). No amplitude self-calibration was done. The final images produced this way are presented in Figs. 2, 4 and 5.

Fig. 2 presents the new 325 MHz image. The angular resolution of this map is  $5.68 \times 4.77$  arcsec at a position angle  $45.17^\circ$ . The dynamic range in the image is 830:1 and the rms noise is  $\simeq 8$  mJy/beam. Fig. 5 shows the 74 MHz map with PT overlaid on top of the 325 MHz map. The resolution of the map is  $25.12 \times 9.75$  arcsec at a position angle  $30.95^\circ$ . The dynamic range in the image is  $\sim 385:1$  with rms noise 0.2 Jy/beam. The quality of the 74 MHz map in particular is limited by the fact that the  $uv$  coverage for the PT link is sparse and not very good near the equator. One can see artifacts near the ends of the lobes in Fig. 5, probably due to residual calibration problems. Fig. 3 shows that the PT baselines hardly touch the VLA ones. Self-calibration cannot get rid of small errors if the baselines from all telescopes do not cross over each other very densely, and this may have led to the artifacts in the map. Though the synthesised beam is highly elongated, the axis of maximum resolution fortunately is aligned nicely with the axis of the jets in Her A, allowing many features to be resolved which were not previously seen at 74 MHz (c.f. Fig. 1, top). Fig. 4 shows the 74 MHz map without the PT link for comparison.

## 4 DISCUSSION

### 4.1 The Radio Characteristics

The total radio power of Her A at 325 and 74 MHz from our observations is  $P_{325 \text{ MHz}} = 1.15 \times 10^{27} \text{ WHz}^{-1} \text{sr}^{-1}$  and  $P_{74 \text{ MHz}} = 4.65 \times 10^{27} \text{ WHz}^{-1} \text{sr}^{-1}$  respectively using a mean spectral index  $\alpha \simeq -1.01$ .

It is clear from comparing Figures 4 and 5 that the addition of the PT-link data has resolved many features in the jets that had only previously been identified at higher frequencies. The extended diffuse emission which forms the ‘cocoon’ is more clearly defined in the PT-link map. At 325 MHz, almost all emission was seen in the old maps within the errors (angular size  $199 \times 68$  arcsec). In the original observations at 74 MHz (Kassim et al. 1993) the source had appeared larger ( $227 \times 95$  arcsec) but with the new PT-link resolution the size is  $185 \times 71$  arcsec, which agrees much better with the 325 MHz result. The flux densities measured from our new maps are  $S_{325 \text{ MHz}} = 206$  Jy and  $S_{74 \text{ MHz}} = 835$  Jy. Direct comparison between Figs. 5, 2 and our 1.4 GHz data shows that all radio emission, faint and bright, young and old, is detected (see also Paper II).

The 325 and 74 MHz images (Figs. 2 and 5) show many of the same bright features on both jets as are seen in the higher resolution 1.4 GHz image. These are identified with the helical- and ring-like structures in the eastern and western side of the radio emission respectively. These features also have flatter spectrum than the surrounding medium and so they belong to the younger material ejected from the nucleus (Gizani & Leahy 2003). Neither map resolves the core

<sup>3</sup> <http://lofar.nrl.navy.mil/pubs/tutorial/>

<sup>4</sup> A “3-D” wide-field imaging technique, which does an interpolation between a set of small overlapping images of multiple pointings, called facets, producing a single image centered on the facet centered on the source.

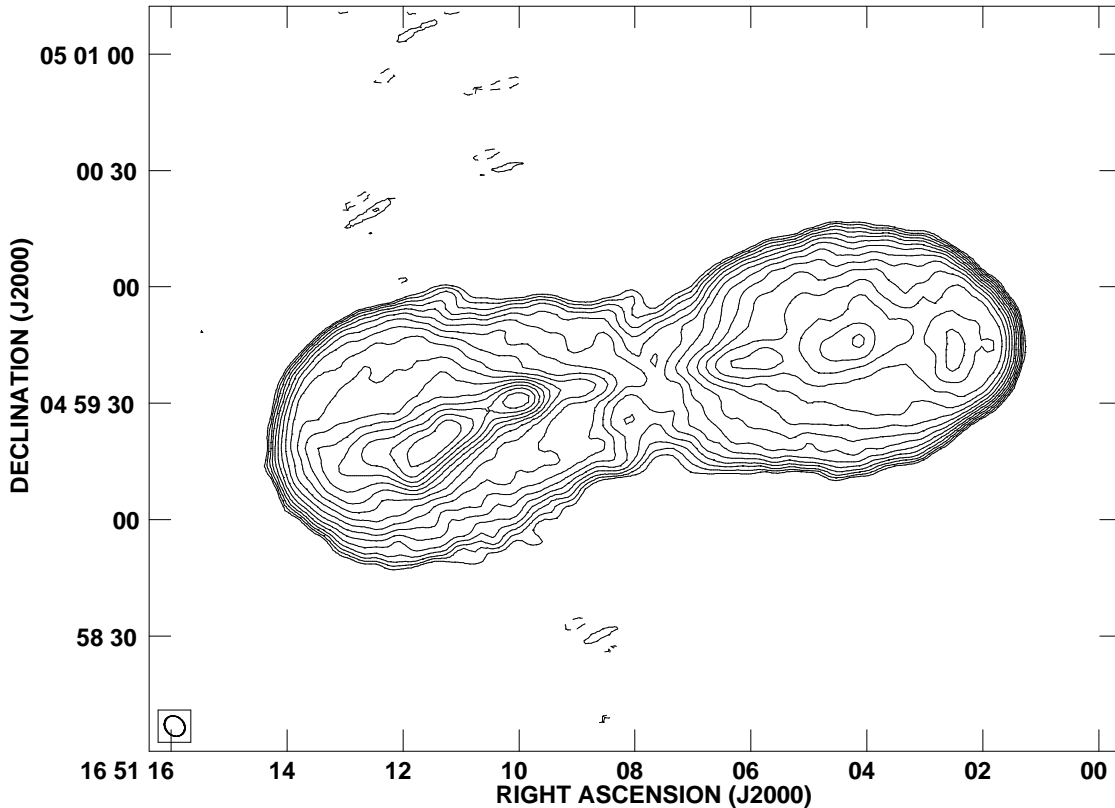


**Figure 2.** The 325 MHz map produced by combining both the A and B array data. The beam size is  $5.68 \times 4.77$  arcsec at a position angle  $45.17$  deg and it is shown in the lower left-hand corner. The dynamic range in the image is 800:1 and the rms noise is  $\approx 8 \text{ mJy beam}^{-1}$ . Contours are separated by factors  $\sqrt{2}$ , starting at  $25 \text{ mJy beam}^{-1}$ . Coordinates are as in Figure 1.

which is found to be very faint and, surprisingly enough, to have a steep spectrum (Gizani & Leahy 2003). Our spectral aging study will be given in a follow-up paper (Gizani, Cohen, Kassim & Leahy, in prep.) where we expect to present a detailed characterization of the spectral curvature. At the current observing frequencies we expect the spectrum to be flatter than at higher frequencies because of the aging of the relativistic particle energy spectrum.

#### 4.2 Spectral Index

We present here the resulting spectral index map from our observations at low frequencies, leaving however the more sophisticated, detailed analysis for a subsequent paper by Gizani et al. in preparation as stated above. Fig. 6 shows the spectral index map between 74 and 325 MHz, i.e. the image of  $\alpha_{74}^{325}$ . We adopt the convention for spectral index  $\alpha$ , flux density  $S_\nu \propto \nu^\alpha$ , where  $\alpha < 0$ .

From this map, the average spectral index of the source is  $\alpha \approx -1.1$ . The image hints at the distinction between the bright and diffuse structures noted by Gizani & Leahy (2003). The former have flatter, younger, spectra and the latter, as well as the overall 'cocoon', have older, steeper spectrum. However the spectral index of the jets and rings is contaminated by the lobe material superposed along the

line of sight, and so the apparent spectral index of the high-brightness features is steeper than the true value.

Gizani & Leahy (2003) interpreted the spectral index differences at high frequency in terms of multiple outbursts which assume spectral curvature. This outburst interpretation is confirmed by our low frequency observations, because the spectral differences between different regions of the radio emission are smaller at the  $\alpha(74, 325)$  map. The spectrum of the inner region curves, as otherwise there would be a lot of emission with  $\alpha < -2.0$  (c.f. Gizani & Leahy (2003)).

The steep spectrum core found by Gizani & Leahy (2003) is hinted in the 325 MHz map (see Fig. 2) and it is basically absent in Fig. 5 at 74 MHz. This absence is not really a resolution problem, since convolving our high resolution stacked map at 1.4 GHz (see Gizani & Leahy 2003) with the 325 MHz beam, still shows the presence of the core. Since the compact core is self-absorbed, we suggest that its subsequent disappearance at lower frequencies is because of spectral curvature occurring at these frequencies.

The relation between the turnover frequency  $\nu_{break}$  (in GHz) versus the projected linear size  $\theta$  (in mas) in a homogeneous, self-absorbed, incoherent synchrotron radio source, when the turnover in the spectrum is due to synchrotron self-absorption, is given by O'Dea & Baum (1997):

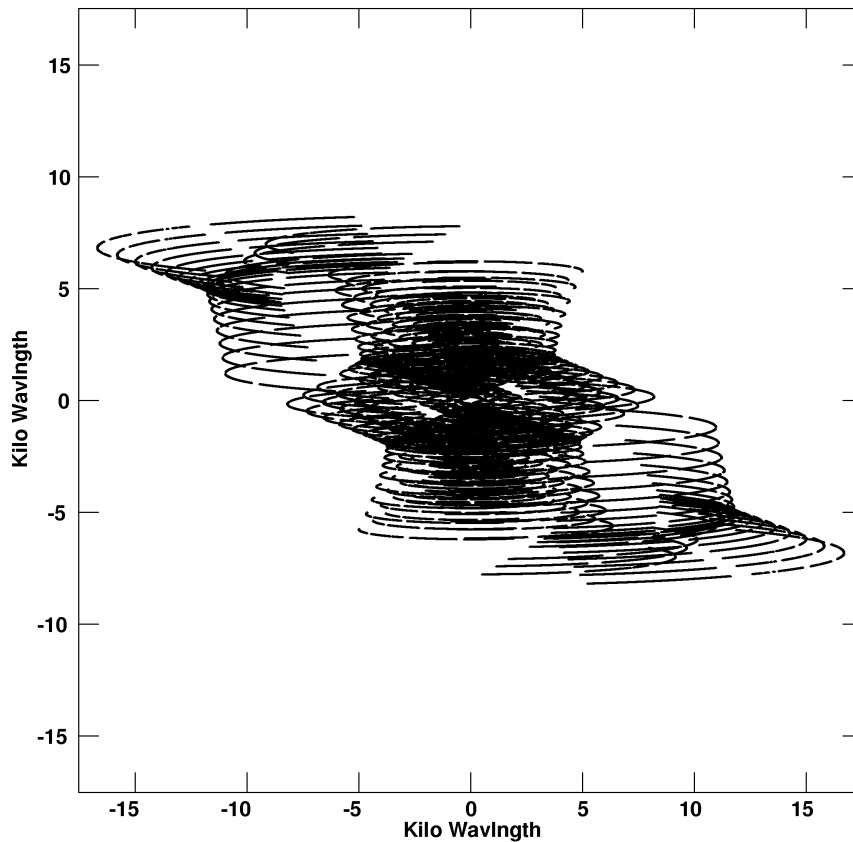


**Figure 3.** The  $uv$ -coverage for the 74 MHz observations of Her A utilizing the PT link. The near equatorial location of Her A causes the long VLA-PT baselines to be mostly in the east-west direction. As a result, the synthesised beam for the VLA-PT link image shown in Figure 5 is elongated, while in the case of all other images we present it is more nearly circular because they did not utilize the PT link. Because the outer regions of the  $uv$ -plane are relatively sparsely covered compared to the inner regions, it was necessary to use nearly uniform weighting to achieve the full resolving power of the VLA-PT link.

$$\theta \simeq 13.45 \left( \frac{S^2 B (1+z)}{\nu_{break}^5} \right)^{\frac{1}{4}}$$

where  $B$  is the magnetic field in Gauss,  $S$  is the flux density at the peak in Jy, and  $z$  is the redshift. For the Hercules A cluster the central magnetic field is of the order of  $\mu\text{G}$  ( $3 \lesssim B_o(\mu\text{G}) \lesssim 9$ , Gizani & Leahy (1999) and in preparation). Assuming that the turnover in the spectrum occurs at 74 MHz where the flux of the compact core is  $\simeq 1090$  mJy, then its size  $\theta$  is estimated to be  $\geq 10$  mas. Gizani, Garrett & Leahy, 2002 and in preparation, using new EVN and MERLIN observations of the core region at 18 cm, revealed emission coming from  $10 \times 20$  mas scales ( $20 \times 50$  pc).

### 4.3 The Radio/X-ray interaction

The analysis of the ROSAT PSPC data suggested that the X-ray emission extends well beyond the radio emission (Gizani & Leahy 2004). The total mass of the cluster at 500 arcsec radius is  $1.5 \times 10^{14} M_\odot$ , and the accretion rate is  $\dot{M} \simeq 15 M_\odot \text{ yr}^{-1}$  (adopting the relation of the cooled mass which should be equal to the heat loss rate over the heat per unit mass Ikebe et al. 1997).

We expect the low frequency radio emission to origi-

nate, most likely, from the oldest electron populations. Our 74 MHz map could clarify if there is any association between the X-ray and radio emission shown as holes (areas empty from X-ray gas) or bright patches (cooler X-ray emitting clouds of gas swept by the radio lobes), or other features pointing to the fossil radio lobes, currently devoid of energetic electrons. However there are no extra regions of radio emission at 74 MHz, so there seems to be no such interaction. Gizani & Leahy, 2004 have shown that the low signal-to-noise ratio HRI data and the low resolution PSPC data are insufficient to reveal a sign of interaction. Our high and low frequency radio observations on Hercules A together with the analysis of the higher resolution and deeper observations by *Chandra* should help clarifying this matter (Wilson et al., 2005, in prep.).

## 5 CONCLUSIONS

We reported on the high resolution VLA observations of Her A employing the newly established VLA-PT link at 74 MHz. We have also presented the new A+B configuration map of the source at 325 MHz. The Her A image at 74 MHz with PT is dramatically different than the one ex-

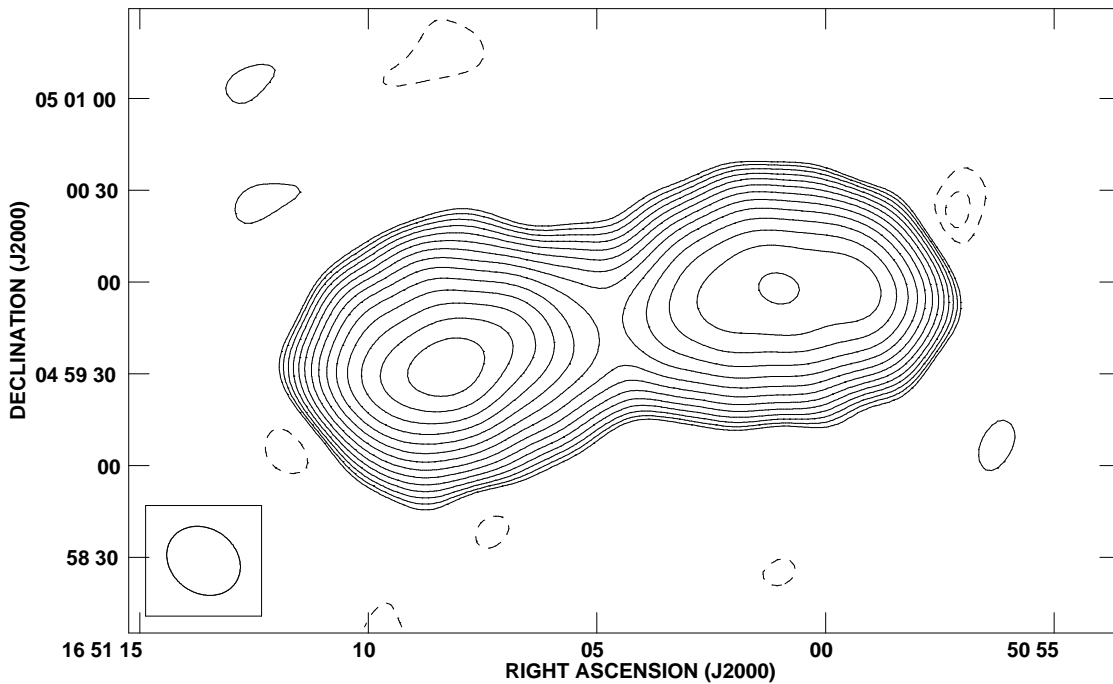


**Figure 4.** The 74 MHz map without the PT link. The beam size is  $(25.4 \times 21.1$  arcsec with  $PA = 55.0$  arcsec) shown in the lower left-hand corner. Contours are separated by factors  $\sqrt{2}$ , and starting at  $0.5$  mJy beam $^{-1}$ . Coordinates are as in Figure 1.

cluding the link. The bright ring-like and helical features in the western and eastern lobe are resolved at the high resolution of  $\approx 10$  arcsec currently provided by the PT link. These structures were not even hinted in the earlier published map at the same frequency. In addition, the new images support the presence of a complicated extended structure and a diffuse well-defined emission. However the ends of the eastern and western lobes suffer from the presence of ripples, probably due to residual self-calibration problems, because the longer PT baselines do not overlap much with the shorter ones. Another reason for the presence of these artifacts could be the limitation in deconvolution induced by the fact that the  $uv$  coverage for the PT link is relatively poor near the equator.

The spectral differences between different regions at high frequency are smaller at low frequency. This is evidence of spectral curvature confirming the multiple outburst interpretation used by Gizani and Leahy (2003), to interpret the presence of regions with different age (with younger and older material) apparent at the spectral index at high frequencies.

The steep spectrum, self absorbed core of Hercules A is absent at 74 MHz. At 325 MHz is barely visible. We suggest that its subsequent disappearance at lower frequencies is because of spectral curvature occurring in these frequencies. We suggest that the likely candidate of the origin of the low frequency spectral curvature of the core is synchrotron self-absorption.

Our low frequency data do not find any extra areas of radio emission so the situation between the radio-X-ray correlation remains as reported in Gizani & Leahy (2004).

Our long track observations for this exceptionally bright source will provide critical input to the ongoing efforts to improve the sophistication of VLA calibration for all low frequency observations, and to extend their application to the PT link. Our observations will enlarge the currently short list of long, uninterrupted track data on bright objects at high resolution in order to explore refractive, differential refractive, and related ionospheric effects, and to gauge the algorithms' ability to correct them on short time scales. Our VLA-PT link Her A image can also be a useful model for future calibration.

#### ACKNOWLEDGMENTS

We acknowledge Paddy Leahy and Rick Perley for helpful discussions. Nectaria Gizani would like to acknowledge the Naval Research Laboratory travel and maintenance grant, with which her travel to the US and data reduction was made possible. NG acknowledges the grant PRAXIS XXI/BPD/18860/98 from the Fundação para a Ciência e a Tecnologia, Portugal for her post-doctoral fellowship of 2002–2003, during which the observations and most of the data reduction of the current work were made; Also the 2004–2007 post-doctoral grant SFRH /BPD/11551/2002, from the same Institute during which this work was published. NG also acknowledges the State Scholarships Foundation (IKY), Greece, for her 2003–2004 post-doctoral grant under contract 332 during which the current paper was written. Finally NG is grateful to the Departamento de Física of the Faculdade de Ciências of the Universidade de Lisboa,

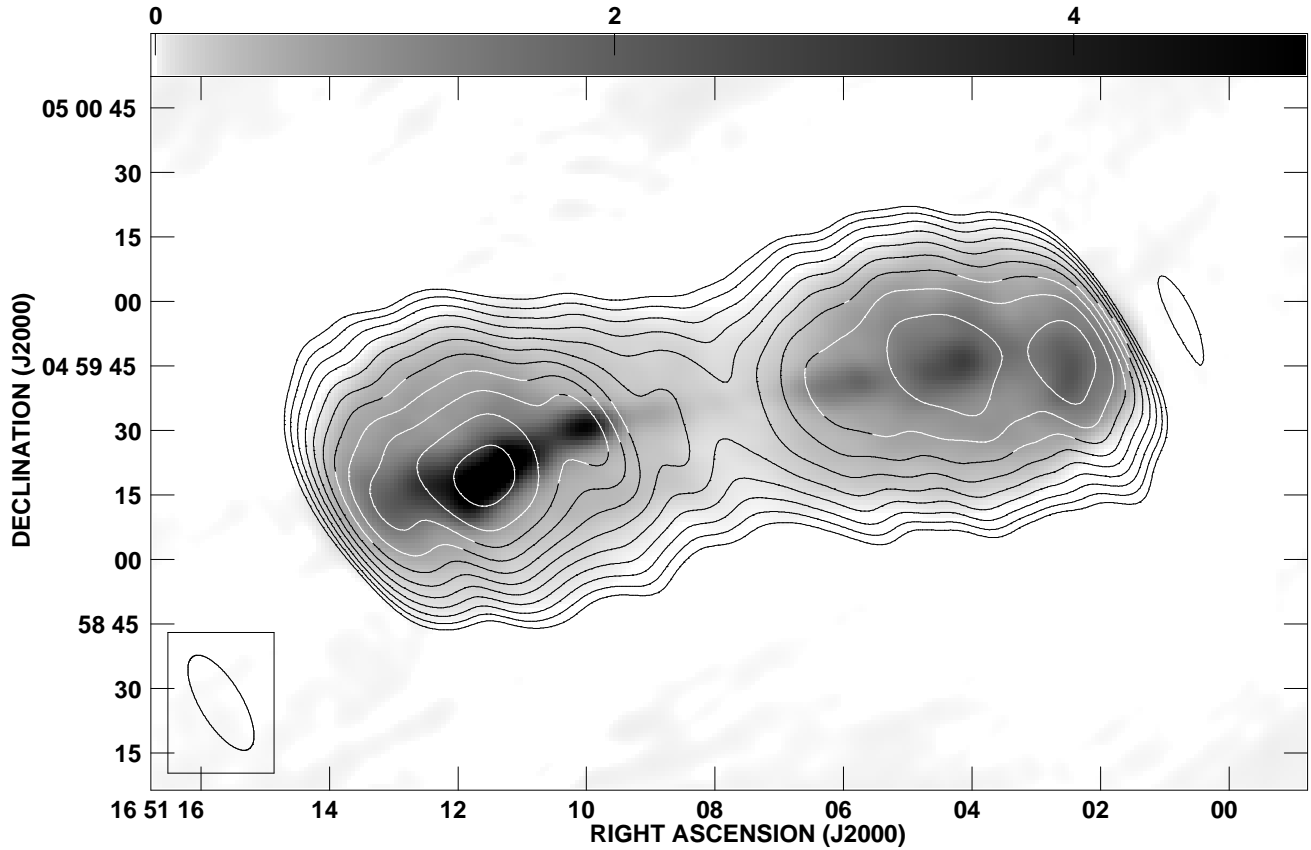


**Figure 5.** The best 74 MHz map with the PT antenna (contours) overlaid on top of the 325 MHz map (grey-scale). The dynamic range in the image is  $\sim 360:1$  with rms noise  $0.2 \text{ Jybm}^{-1}$ . The beam size ( $25.12 \times 9.75$  arcsec,  $\text{PA} = 30.95^\circ$ ) is shown in the lower left-hand corner. Contours are separated by factors  $\sqrt{2}$ , and starting at  $\pm 2 \text{ Jy/beam}$ . Coordinates are as in Figure 1.

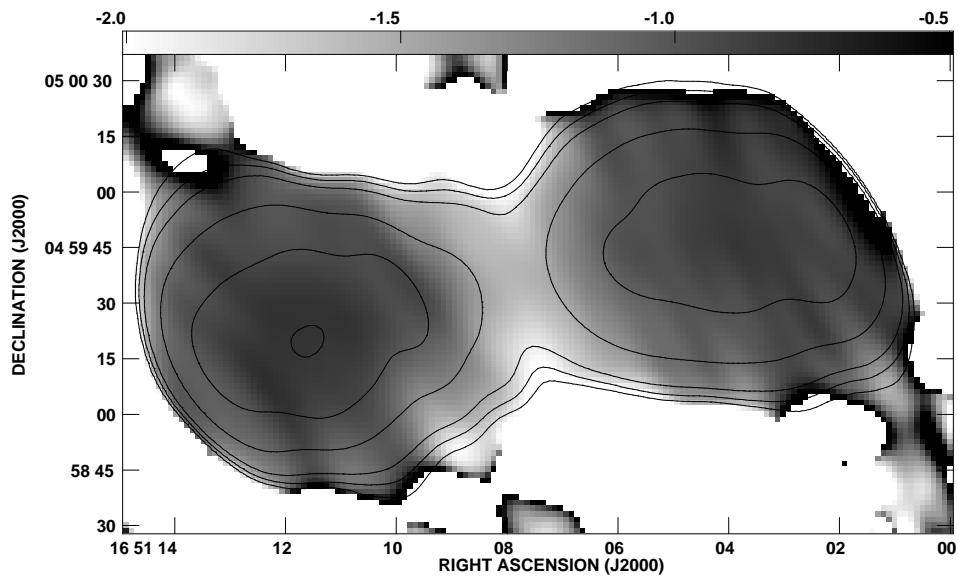


**Figure 6.** Grey-scale of the spectral index map between 74 and 325 MHz at  $25.12 \times 9.75$  arcsec resolution with  $\text{PA} = 30.95^\circ$ . The grey-scale runs from  $-2.5 \leq \alpha \leq -0.5$ . Contours are of the 325 MHz map at the 74 MHz resolution, separated by factors of 2 starting at  $\approx 81 \text{ mJy beam}^{-1}$ .



Portugal for allowing her to use its installations to carry out this task.

Basic research in astronomy at the NRL is funded by the Office of Naval Research. The National Radio Astronomy Observatory is a facility of the National Science Foundation operated under cooperative agreement by Associated Universities, Inc. This research has made use of the NASA/IPAC Extragalactic Database (NED) which is operated by the Jet Propulsion Laboratory, Caltech, under contract with the National Aeronautics and Apace Administration. This research has also made use of NASA's Astrophysics Data System.

## REFERENCES

- Bennett, C. L., et al., 2003, ApJS, 148, 1  
Dreher J. W., Feigelson E. D., 1984, Nat, 308, 43  
Erickson W. C., Mahoney M.J., Erb K., 1982, ApJS, 50, 403  
Fanaroff B., Riley J. M., 1974, MNRAS, 167, 31P  
Gizani N. A. B., Leahy J. P., 1999, NewAR, 43, 639  
Gizani N., Garrett M. A., Leahy J. P., 2002, Publ. astron. Soc. Australia, 19, 69  
Gizani N. A. B., Leahy J. P., 2003, MNRAS, 342, 399 (astro-ph/0305600)  
Gizani N. A. B., Leahy J. P., 2004, MNRAS, 350, 865 (astro-ph/0402072)  
Hewish, A. 1952, Royal Society of London Proceedings Series A, 214, 494  
Ikebe Y., Makishima K., Ezawa H., Fukazawa Y., Hirayama M., Honda H., Ishisaki Y., Kikuchi K., Kubo H., Murakami T., Ohashi T., Takahashi T., Yamashita K., 1997, ApJ, 481, 660  
Jansky, K. G., 1933, Proc. IRE, vol. 21, pp. 1387-1398, October, 1933  
Kassim N. E., Perley R. A., Erickson W. C., Dwarkanath K. S., 1993, AJ, 106, 2218  
Kassim, N. E., Lazio, T. J. W., Erickson, W. C., Crane, P. C., Perley, R. A., & Hicks, B. 2002, IAU Symposium, 199, 474  
Kassim, N. E., Lazio, T. J. W., Erickson, W. C., Perley, R. A., Cotton, W. D., Greisen, E. W, Hicks, B., Cohen, A. S., Lane, W. M., & Rickard, L. J. 2004, "The 74 MHz System on the Very Large Array", ApJS, submitted  
Leahy J. P., 1991, in Hughes P. A., ed., *Beams and Jets in Astrophysics* C.U.P., Cambridge, p. 118  
O'Dea, C. P., & Baum, S.A., 1997, AJ, vol. 113, p. 148  
Reber, G., 1940, ApJ, vol. 91, p. 621-624  
Rees N., 1990, MNRAS, 244, 233  
Ryle, M. & Smith, F. G., 1948, Nature, vol. 162, p. 462